Neurobiology of Stress 15 (2021) 100418

Contents lists available at ScienceDirect

Neurobiology of Stress

journal homepage: www.elsevier.com/locate/ynstr

Stronger functional network connectivity and social support buffer against negative affect during the COVID-19 outbreak and after the pandemic peak

Mingyue Xiao [a,b,1], Ximei Chen [a,b,1], Haijing Yi [a,b], Yijun Luo [a,b], Qiaoling Yan [a,b], Tingyong Feng [a,b], Qinghua He [a,b], Xu Lei [a,b], Jiang Qiu [a,b], Hong Chen [a,b,*]

[a] Key Laboratory of Cognition and Personality (SWU), Ministry of Education, Chongqing, China
[b] Department of Psychology, Southwest University, Chongqing, China

ARTICLE INFO

Keywords:
Negative affect
COVID-19 pandemic
Social support
Salience network
Frontoparietal network
Default mode network

ABSTRACT

Health and financial uncertainties, as well as enforced social distancing, during the COVID-19 pandemic have adversely affected the mental health of people. These impacts are expected to continue even after the pandemic, particularly for those who lack support from family and friends. The salience network (SN), default mode network (DMN), and frontoparietal network (FPN) function in an interconnected manner to support information processing and emotional regulation processes in stressful contexts. In this study, we examined whether functional connectivity of the SN, DMN, and FPN, measured using resting-state functional magnetic resonance imaging before the pandemic, is a neurobiological marker of negative affect (NA) during the COVID-19 pandemic and after its peak in a large sample (N = 496, 360 females); the moderating role of social support in the brain-NA association was also investigated. We found that participants reported an increase in NA during the pandemic compared to before the pandemic, and the NA did not decrease, even after the peak period. People with higher connectivity within the SN and between the SN and the other two networks reported less NA during and after the COVID-19 outbreak peak, and the buffer effect was stronger if their social support was greater. These findings suggest that the functional networks that are responsible for affective processing and executive functioning, as well as the social support from family and friends, play an important role in protecting against NA under stressful and uncontrollable situations.

1. Introduction

The coronavirus disease 2019 (COVID-19) has presented humanity with one of the greatest global health and economic crises in the 21st century and has increased people's negative moods, including worry, stress, sadness, despair, and fear. Poor psychological state and high anxiety were found in the general Chinese population in the early phase of the COVID-19 outbreak (Qian et al., 2020; Ren et al., 2020). Moreover, several recent longitudinal studies focusing on psychologically related distress during different COVID-19 phases have found no change in negative emotions, such as anxiety and depression, between the initial outbreak and the after-peak period in China (C. Wang et al., 2020; Y. Wang, Hu, Feng, Wilson and Chen, 2020), suggesting that the mental health consequences of the COVID-19 pandemic could last over time and that mental health problems could peak later than the actual pandemic (Gunnell et al., 2020). Considering the enormously uncertainty, life-threatening conditions, and the continued loss due to the pandemic, the impact of COVID-19 is expected to be detrimental to mental health both during and after the pandemic (Galea et al., 2020; Holmes et al., 2020). Therefore, it is crucial to investigate neurobiological and social protective factors that buffer against the influence of negative affect (NA) not only during but also after the COVID-19 peak period.

Many previous studies on the neural mechanism of NA have demonstrated that regions in the salience network (SN) (e.g., dorsal anterior cingulate cortex [dACC] and insula) are involved in the processes of conflict resolution, emotional awareness, and regulation (Craig, 2009; Johnstone et al., 2007; Kerns et al., 2005). Some brain regions of the default mode network (DMN), such as the medial prefrontal cortex (mPFC), posterior cingulate cortex (PCC), and precuneus, are associated with negative emotional processes (Andrews-Hanna,

* Corresponding author. Key Laboratory of Cognition and Personality, Ministry of Education, Faculty of Psychology, Southwest University, Tiansheng Road No.2, Beibei District, Chongqing, China.
E-mail address: chenhswu@163.com (H. Chen).
[1] Mingyue Xiao and Ximei Chen contributed equally to this work.

https://doi.org/10.1016/j.ynstr.2021.100418
Received 1 August 2021; Received in revised form 27 September 2021; Accepted 15 November 2021
Available online 16 November 2021

2012; Greicius et al., 2003; Raichle et al., 2001; Veer et al., 2011). The PFC of the frontoparietal network (FPN) is also crucial to negative emotional processes since it is associated with cognitive control and emotion regulation (Drabant et al., 2009; Ochsner and Gross, 2005; Quirk and Beer, 2006). In addition, accumulating studies have attempted to identify the functional connectivity (FC) of negative emotion with task-based and resting-state data (Elmira et al., 2018; Harrison et al., 2008; Lydon-Staley et al., 2019). Notably, several meta-analysis studies have suggested that abnormal FCs within and between the SN, DMN, and FPN are associated with affective-related psychopathologies (Z. He et al., 2019; Kaiser et al., 2015; Xu et al., 2019). Researchers in Stanford University have proposed that interactions among the SN, DMN, and FPN constitute the Triple Network Model of psychopathology (V. Menon, 2011). These three networks are considered to function in an interconnected manner and participate in higher information processing of the entire internal and external environment of the organism to determine which behavioral strategy should be adopted during the processes of emotional response and regulation (B. Menon, 2019). Specifically, the SN functions as a switch between the FPN and the DMN suppressing the latter and activating the former when a salient stimulus occurs. Failure of this switch would lead to impaired detection and mapping of salient external stimuli and internal events, with significant consequences for both cognitive control and self-monitoring. In other words, weak mapping from the SN gives rise to aberrant engagement of the FPN and DMN, which would compromise cognition and goal-relevant adaptive behavior, as well as alter the self-referential mental activity (e.g., excessive rumination in patients with depression) (V. Menon, 2011; Miller and Cohen, 2001; Seth, 2005). In addition, aberrant communication between the FPN and DMN may reflect ongoing rumination or an underlying bias for control systems (Roselinde H Kaiser et al., 2015a,b). Previous studies have reported that greater strength of connectivity between the DMN and FPN is associated with poorer cognitive control performance and more repetitive negative thinking (Hampson et al., 2010; Lydon-Staley et al., 2019). Taken together, these findings suggest that the negative emotional response and regulation processes are associated with alterations of multiple brain regions in the SN, DMN, and FPN functional networks.

Given that the emotional state is affected by the interaction of the brain and environment (Schmidt et al., 2010; Schmidt et al., 2010), the influence of social support on the pandemic-related NA level under COVID-19 social isolation should be focused on. Numerous studies have indicated that social support is an essential resource for coping with adversity and maintaining physical and psychological health (d'Arbeloff et al., 2018; Michalak et al., 2003; Ozbay et al., 2007; Palinkas et al., 2004; Resick, 2001). The National Cancer Institute defines social support as "a network of family, friends, neighbors, and community members that is available in times of need to give psychological, physical, and financial help" (www.cancer.gov). According to the stress-buffering hypothesis (Cohen and McKay, 2020; Cohen and Wills, 1985), social support moderates the relationship between NA or stress and the physiological reaction (Giesbrecht et al., 2013; Puterman et al., 2014), such as the amygdala action (Hyde et al., 2011). Thus, identifying the buffering impact of social support on NA might be crucial for improving people's mental health during and after the COVID-19 pandemic.

Previous neuropsychological studies have advanced our understanding of the neural basis of NA in routine life. Many studies have also explored the neural mechanism of the negative mental state during the COVID-19 pandemic (Chahal et al., 2021; L. He et al., 2021; Liu et al., 2021). However, to the best of our knowledge, no study has used resting-state functional connectivity (rsFC) to predict NA at the different stages of the COVID-19 pandemic in healthy people. More importantly, to date, no effort has been made to identify a protective factor that moderates the relationship between the neural mechanism and the mental symptoms.

Thus, in the present study, we used the intrinsic rsFC, which is a powerful indicator for detecting spontaneous brain activity and investigating the neural bases underlying behavior at the individual level (Biswal, 2012; Kunisato et al., 2011; Lei et al., 2015), to identify the inherent brain functional networks, i.e., resting-state networks (RSNs) (Dijk et al., 2010). We determined whether social support moderates the association between rsFC of the SN, DMN, and FPN before the COVID-19 (T1) outbreak and NA levels during the COVID-19 outbreak and after the peak period. Based on previous studies (Chahal et al., 2021; L. He et al., 2021; C. Wang et al., 2020; Y. Wang et al., 2020), we expected that, on average, participants would report higher NA levels during the pandemic than before the pandemic, and that the NA level would not decrease immediately after the pandemic outbreak peak (hypothesis 1). According to literatures mentioned above, we hypothesized that greater connectivity of intra-SN, SN−FPN, and SN−DMN, as well as the decreased connectivity of FPN−DMN are associated with the reduced NA brought by the COVID-19 pandemic (hypothesis 2). Importantly, we expected that social support moderates this neural-NA association, and individuals with a higher level of social support would show stronger correlations between network connectivity and NA (hypothesis 3).

2. Methods and materials

2.1. Participants

Data were derived from the "Behavioral Brain Research Project of Chinese Personality" (BBP). A three-wave panel study was conducted over an 8-month period. Specifically, before the pandemic (September 17, 2019–January 11, 2020, T1), participants of the BBP had completed the NA measurement before and after resting-state fMRI scanning. On January 23, 2020, China imposed a lockdown in Wuhan to quarantine the center of an outbreak of COVID-19. On February 17, 2020, the number of existing confirmed cases reached its peak in China. A total of 901 undergraduates from the BBP were recruited via mobile telephone text message to complete the first online pandemic questionnaire survey from February 22 to 28, 2020 (T2). On April 8, 2020, the Wuhan lockdown officially ended. The second online pandemic questionnaire survey was performed during the remission period of the pandemic (April 24−May 1, 2020, T3). In total, 496 participants with pre-pandemic brain imaging data and pandemic-related NA scores in the two stages of the pandemic were included in the present analysis (360 females, mean age = 19.22 years; standard deviation (SD) = 0.86, age range = 17–26 years).

All participants were college students in Southwest China, and none reported a history of psychiatric or neurological illnesses. All participants signed informed consent forms before participating in the study and were monetarily compensated at the end of the study. Ethical approval for this study was granted by the Ethics Committee of the University, and all procedures involved were in accordance with the sixth revision of the Declaration of Helsinki.

2.2. Measures

2.2.1. The NA questionnaire (T1, T2, and T3 assessments)

We used eleven items to assess the negative emotions experienced, including distressed, upset, guilty, scared, hostile, irritable, alert, ashamed, nervous, jittery, and afraid. The factor structure of the 11-item negative emotional scale replicates the original Positive and Negative Affect Schedule factor structure (Watson et al., 1988) in Chinese samples (Jackson and Chen, 2015). To be attention, this scale included alert as a negative emotion rather than positive, as alert has negative meaning in Chinese language and culture. Items were rated from 1 (not at all) to 5 (very much). The average score of NA measured before and after the resting-state fMRI scanning was computed and used as a baseline of NA. In this study, the Cronbach's alpha of the NA in different stages ranged 0.90–0.93.

2.2.2. The Social Support Scale (T2 assessment)

The scale of perceived social support (X. Wang, Wang and Ma, 1999) is a 12-item measure that assesses participants' perceived social support (e.g., "when I have problems, some people [i.e., relatives, friends, classmates] were there accompanying me"). Responses were rated on a 5-point Likert-type scale (1 = never to 5 = always). Cronbach's alpha of the Social Support Scale in the current study was 0.94.

2.3. rsfMRI data acquisition and preprocessing

2.3.1. Image acquisition (T1 assessment)

For each participant, rsfMRI scanning was performed with a 3 T Prisma Siemens Trio MRI scanner (Siemens Medical Systems, Erlangen, Germany) using a 32-chanel brain coil. We used a gradient echo-planar imaging sequence to obtain the resting-state functional image, and the scanning parameters were as follows: repetition time (TR) = 2000 ms; echo time (TE) = 30 ms; slices = 62; slice thickness = 2 mm; field of view read = 224 × 224 mm^2; flip angle = 90°; resolution matrix = 112 × 112; voxel size = 2 × 2 × 2 mm^3; phase encoding direction = PC » AC. Each section contained 240 volumes. High-resolution T1-weighted structural images were acquired for coregistration purposes (parameters: TR = 2530 ms; TE = 2.98 ms; field of view read = 256 × 256 mm^2; flip angle = 7°; base resolution = 256 × 256; slice per slab = 192; slice oversampling = 33.3%; voxel size = 0.5 × 0.5 × 1 mm^3; phase encoding direction = AC » PC).

2.3.2. Image data preprocessing

Data Processing & Analysis for (Resting-State) Brain Imaging (Yan et al., 2016), based on the statistical parametric mapping software (SPM8, http://www.fil.ion.ucl.ac.uk/spm), was used to preprocess the image data. The preprocessing was conducted as follows. The first 10 images were discarded to allow for participant familiarization and fMRI-signal stabilization. The remaining images were corrected for temporal shifts between slices and realigned to the middle volume. Next, using the EPI templates in SPM8 (Ashburner, 2007), each image volume was spatially normalized to the Montreal Neurological Institute (MNI) 152-brain template, with a resolution voxel size of 3 × 3 × 3 mm^3. The images were then spatially smoothed with a 4-mm full width at half maximum Gaussian kernel, and linear trends were subsequently removed. We regressed nuisance signals (including white matter, cerebrospinal fluid, and head-motion parameters) and their derivatives using a Friston 24-parameter model to control for potential physiological effects (Friston et al., 1996; Hallquist et al., 2013). Linear and quadratic trends were also included as regressors, because the blood-oxygen-level-dependent signal exhibits low-frequency drifts. To remove the effects of very-low-frequency drifts and high-frequency noises, all images were filtered using a temporal band-pass filter (0.01–0.08 Hz).

During scanning, each participant was asked to remain still and relaxed, with eyes closed, and not think of anything deliberately. Foam pads and earplugs were employed to reduce head motion and scanning noise. In final formal analysis, no participant had head motion of >2.0 mm in any direction between volumes, rotation of >2.0 in any axis during scanning, or mean framewise displacement (FD) of >0.50 (Chen et al., 2021; Tie et al., 2015).

2.4. Data analysis

2.4.1. Functional network connectivity (FNC) analysis

The FC within and between the three RSNs that correlate with NA was assessed on the network level using the CONN toolbox, version 17f (Whitfield-Gabrieli and Nieto-Castanon, 2012). The connectivity strength between the 17 regions of interest (ROIs; brain regions indicated in parentheses) of the following three RSNs was included in the analysis: DMN (mPFC, bilateral lateral parietal cortex, and PCC [this ROI also covers parts of the precuneus]), SN (dACC, bilateral anterior insula [AI], bilateral rostral PFC, bilateral supramarginal gyrus [SMG], and bilateral amygdala), FPN (bilateral dorsolateral PFC [dlPFC] and bilateral posterior parietal cortex [PPC]). All the 17 ROIs were derived from the CONN toolbox. The bilateral amygdala ROIs were derived from the FSL Harvard-Oxford Atlas maximum likelihood subcortical atlas (Desikan et al., 2006; Schouten et al., 2016; Van Duijvenvoorde, Westhoff, de Vos, Wierenga and Crone, 2019), while the other ROIs were defined from CONN's ICA analyses of the HCP dataset (497 subjects) (W. Shen et al., 2019; Wehrle et al., 2018; Whitfield-Gabrieli and Nieto-Castanon, 2012) (for peak MNI coordinates and images of these ROIs, see Table S1 and Fig. S1). To produce first-level correlation maps for each participant, the average BOLD time series for all voxels in each seed ROI was extracted and Fisher z-transformed. Then, pairwise bivariate correlation coefficient (i.e., Pearson's correlation), which is computationally less expensive and preferable for large datasets (Mahadevan et al., 2021), was calculated using the time courses for each of the ROI, producing a symmetrical 17 × 17 correlation matrix (i.e., ROI-to-ROI connectivity matrix). At the second level, the resultant correlation coefficients were further correlated with NA scores using multiple regression analyses to test the relationship between FNC and negative emotion. For these analyses, we used a false discovery rate (FDR) corrected threshold of $p < 0.05$ (two-sided). This correction was applied at the seed level, after testing for connectivity between all seed-target ROI pairs in the given network. In these analyses we included age, sex, mean FD, and the NA level of baseline as covariates of no interest to ensure that our results only revealed FC correlations and differences uniquely explained by NA and not attributable to differences in age, sex, head motion, or the emotional state during scanning. Finally, the mean connectivity strength values (Z-scores) within and among the three networks was calculated based on the ROI-to-ROI connectivity that correlated with NA (Chen et al., 2021; Domakonda et al., 2019).

2.4.2. Prediction analysis

This study conducted a traditional regression analysis to test the relationship between resting-state networks and NA scores. We treated the average FC values within or between the three networks as the independent variable, NA (T2) or NA (T3) as the dependent variable. Age, sex, FD and the NA level of baseline were set as controlling variables. Notably, given that the machine learning approach allows for the prediction of unseen participants, offering information at the individual level rather than group level (Cui et al., 2018; X. Shen et al., 2017; Yarkoni and Westfall, 2017), and given that a ten-fold cross-validation may provide more stable estimates of predictive performance (Varoquaux et al., 2017), we further performed a machine-learning method named linear support vector regression (SVR) and ten-fold cross--validation (Beaty et al., 2018; Supekar et al., 2013) to test the robustness of the brain-behavior relationship. We divided the data randomly into ten folds, and used nine folds to build a linear regression model which we subsequently tested on the tenth fold data. In the linear regression algorithm, the NA scores (T2 and T3) were taken as the dependent variables respectively and the corresponding functional network connectivity (i.e., the mean within- and between-network connectivity values) was taken as the independent variable. After repeating this procedure ten times, we obtained the predicted NA scores (T2 and T3) of each participant. The predictive power of the model was assessed by the magnitude and statistical significance of Pearson's correlation between actual and predicted behavioral values. If actual and predicted NA scores were significantly positively related, this would indicate that the model was successful in its prediction. Then, permutation testing was used to test the significance of the prediction results. We randomly shuffled the label between observed NA scores (T2 and T3) and functional network connectivity each time and reran the above ten-fold prediction procedure. The 5000 Pearson correlations between observed and predicted scores composed null distributions of r values. The number of null r values was greater than the observed r value and was then divided by 5000, providing an estimated p value.

2.4.3. Moderation analyses

To investigate the role of social support, we carried out moderation analyses using the PROCESS macro in SPSS (Hayes, 2013). We first treated the average FC values within or between the three networks as the independent variable, NA (T2) or NA (T3) as the dependent variable, and social support as the moderator variable. Age, sex, and FD were set as controlling variables. All variables were standardized prior to analysis. The significance of the moderating effect was assessed using a bootstrapping method with 5000 iterations. If the 95% confidence interval (CI) did not contain zero, the moderating effect was considered significant. We employed the Johnson-Neyman technique to quantify the moderation effect, which investigates the strength of the relationship between the predictor and outcome variable across the spectrum of possible values of the moderating variable, and identifies the values of the moderating variable at which this relationship either becomes, or ceases to be, significant (Hayes and Matthes, 2009; Spiller et al., 2013).

2.4.4. Exploratory analyses

Association between network connectivity and specific NA items at T2 and T3. After the aforementioned FNC analyses provided significant connectivity, the mean within-network connectivity and mean cross-network connectivity were calculated by averaging ROI-to-ROI pairwise correlations in/across each network (Chen et al., 2021; Domakonda et al., 2019). Pearson's correlations of mean network connectivity with specific NA items at T2 and T3 were further assessed while correcting for age, sex, FD, and NA (T1) using partial correlation. Statistical analyses were performed using SPSS.

Sex differences in network connectivity associated with NA. Potential sex differences in FNC associated with NA scores were further assessed using an analysis of covariance model (i.e., comparing regressions of the male and female groups) implemented in the CONN toolbox. Statistical significance was set at $p < 0.05$ with FDR correction. Age, FD, and NA (T1) were defined as covariates of no interest.

Associations between whole brain network connectivity and NA. To explore the effects of whole-brain network connectivity patterns on NA, we further performed the whole brain analysis with the DMN (4 ROIs), sensorimotor network (SMN; 3 ROIs), visual network (VN; 4 ROIs), SN (9 ROIs), dorsal attention network (DAN; 4 ROIs), FPN (4 ROIs), language network (LN; 4 ROIs), and cerebellar network (CN; 2 ROIs). All the ROIs were defined from CONN's ICA analyses of the HCP dataset (497 subjects). The covariates and statistical thresholds were the same as those mentioned in the FNC analyses section above.

2.4.5. Sensitivity analyses

Sensitivity analyses using other definitions of RSN were carried out to assess the sensitivity of the current ROI (i.e., SN, DMN, and FPN). Specifically, the ROI for the left and right executive control network (CEN, 12 ROI), the anterior and posterior SN (19 ROI), and dorsal and ventral DMN (19 ROI) were defined based on the well-established freely available atlas of regions defined by correlated activation patterns (http://findlab.stanford.edu/functional_ROIs.html) (Chen et al., 2021; Shirer et al., 2012). The analyses to test network connectivity in relation to NA scores were the same as those mentioned in the functional network connectivity analyses section.

3. Results

3.1. Sample description and behavioral results

Descriptive statistics and correlation analysis for age, FD, and behavioral variables are listed in Table 1. Paired-sample *t*-test showed that NA was significantly higher during ($t = -15.31$, $p < 0.0001$) and after ($t = -14.89$, $p < 0.0001$) the COVID-19 peak than before the pandemic. However, there was no significant difference between during and after the COVID-19 peak in NA measurement ($t = -0.51$, $p = 0.61$). The score differences for each item at the two stages of the pandemic are described in Table S2 and Fig. S2. Sex differences were significant in NA (T2) (female = 2.38 ± 0.77; male = 2.12 ± 0.78; t = 3.21, $p < 0.005$) but not in NA (T3) (female = 2.36 ± 0.80; male = 2.24 ± 0.87; t = 1.50, $p > 0.05$) (see Fig. S3). The correlation between age and NA (T2) was significant ($r = 0.10$, $p < 0.05$) but not that with NA (T3) ($r = 0.003$, $p > 0.05$). We set sex, age, FD, and NA (T1) as the control variables in the further analysis.

3.2. Functional network connectivity analysis

To reveal the relationships between the current networks and NA under COVID-19 conditions, we correlated the NA levels (T2 and T3) with the FNC within and between the three networks. NA (T2) was negatively related to FC within the SN and between the SN and DMN, SN and FPN, and DMN and FPN (Table 2 and Fig. 1). We also found that NA (T3) was negatively related to FC within the SN and between the SN and FPN (Table 3 and Fig. 2). Within-network and between-network correlation matrices are shown in Fig. S5. We also test that whether the within-system connectivity generally is greater than between-system connectivity (Tables S5 and S6).

3.3. Prediction results

The associations between the resting-state networks and NA were tested by performing the regression analyses and results showed that functional network connectivity significantly predicted the NA scores (effect on NA (T2) ranged from −0.22 to −0.12, t-values ranged from −4.80 to −2.83, $p < 0.005$; effect on NA (T3) ranged from −0.15 to −0.14; t-values ranged from −3.31 to −3.18; $p < 0.002$). The results of SVR showed a close relationship between NA (T2) and functional network connectivity [$r_{(\text{predicted, observed})} = 0.191$, $p < 0.001$, see Fig. 3a], as well as between NA (T3) and functional network connectivity [$r_{(\text{predicted, observed})} = 0.152$, $p < 0.001$, see Fig. 3b]. The qualitatively similar results provided added confidence in the robustness of our findings.

3.4. The moderation models

The 5000 bootstrap simulations suggested that social support moderated the relationship between SN–DMN connectivity and NA (T2) (interaction effect = −0.09, 95% CI = [−0.171, −0.004], $p < 0.05$) The moderation effect was quantified using the Johnson-Neyman analysis. The range of simple slopes provided by the Johnson-Neyman analysis demonstrated that the relationship between SN–DMN connectivity and

Table 1
Descriptive statistics and correlation analysis (N = 496).

Variables	Range	Mean	SD	1	2	3	4	5
1 Age	16.62–25.89	19.22	0.86	1				
2 FD	0.02–0.26	0.05	0.03	0.01	1			
3 NA (T1)	1–3.73	1.76	0.55	−0.02	0.04	1		
4 NA (T2)	1–4.18	2.31	0.78	0.10*	−0.03	0.33**	1	
5 NA (T3)	1–4.09	2.33	0.82	0.00	−0.05	0.29**	0.53**	1
6 SS (T2)	1.33–5	3.45	0.73	−0.02	0.10*	−0.03	−0.09*	−0.21**

Note: *$p < 0.05$; **$p < 0.01$. Abbreviations: N = number; SD = standard deviation; FD = framewise displacement; NA = negative affect; SS = social support.

Table 2
Functional connectivity within the SN, and among the three examined networks: Negative correlations with NA (T2) scores[a].

Functional network connectivity	*t*-values	*p*-values[b]	Connectivity value (*Z*-scores)[c]
(a) Within SN			
SN.ACC−SN.SMG (R)	−3.92	0.0016	0.34 (±0.25)
SN.Amyg (R)−SN.rPFC (L)	−3.59	0.0030	−0.01 (±0.21)
SN.SMG (R)−SN.rPFC (L)	−3.05	0.0095	0.36 (±0.27)
SN.Amyg (R)−SN.ACC	−3.10	0.0108	0.08 (±0.22)
SN.AI (L)−SN.SMG (R)	−2.90	0.0369	0.38 (±0.28)
SN.Amyg (R)−SN.rPFC (R)	−3.01	0.0110	−0.03 (±0.21)
SN.ACC−SN.SMG (L)	−2.90	0.0208	0.33 (±0.26)
SN.Amyg (L)−SN.AI (R)	−2.90	0.0410	0.21 (±0.22)
SN.Amyg (R)−SN.AI (R)	−2.67	0.0210	0.20 (±0.23)
SN.Amyg (L)−SN.ACC	−2.66	0.0410	0.10 (±0.22)
SN.Amyg (L)−SN.rPFC (R)	−2.58	0.0410	−0.03 (±0.21)
(b) Between SN and FPN			
SN.Amyg (R)−FPN.dlPFC (R)	−3.91	0.0017	0.03 (±0.20)
SN.SMG (R)−FPN.PPC (L)	−2.92	0.0103	0.08 (±0.26)
SN.AI (L)−FPN.dlPFC (R)	−2.85	0.0369	0.21 (±0.26)
SN.Amyg (L)−FPN.dlPFC (R)	−2.69	0.0392	0.02 (±0.20)
SN.AI (R)−FPN.dlPFC (L)	−2.64	0.0456	0.21 (±0.25)
SN.AI (L)−FPN.PPC (L)	−2.66	0.0427	0.30 (±0.24)
SN.Amyg (R)−FPN.PPC (L)	−2.72	0.0210	0.01 (±0.20)
SN.Amyg (R)−FPN.dlPFC (L)	−2.51	0.0248	0.05 (±0.21)
(c) Between SN and DMN			
SN.SMG (R)−DMN.lPC (L)	−3.26	0.0094	−0.01 (±0.29)
SN.SMG (R)−DMN.lPC (R)	−3.11	0.0095	0.03 (±0.31)
SN.SMG (L)−DMN.lPC (R)	−2.79	0.0435	0.12 (±0.29)
SN.SMG (R)−DMN.mPFC	−2.62	0.0205	−0.17 (±0.29)
SN.Amyg (R)−DMN.PCC	−2.54	0.0248	0.19 (±0.19)
(d) Between DMN and FPN			
FPN.PPC (L)−DMN.PCC	−2.83	0.0320	0.23 (±0.22)

Abbreviations: NA = negative affect; SN = salience network; DMN = default mode network; FPN = frontoparietal network; Amyg = amygdala; rPFC = rostral prefrontal cortex; dACC = dorsal anterior cingulate cortex; AI = anterior insula cortex; SMG = supramarginal gyrus; dlPFC = dorsolateral prefrontal cortex; PPC = posterior parietal cortex; mPFC = medial prefrontal cortex; PCC = posterior cingulate cortex; lPC = lateral parietal cortex.

[a] Table 2 only shows the significant results (N = 496).

[b] False discovery rate (FDR) seed-level corrected $p < 0.05$, two-sided.

[c] Values are mean ± standard deviation (SD).

NA (T2) was not significant for social support scores of 3.10 or below. However, once social support scores passed this threshold, the relationship between SN–DMN connectivity and NA (T2) was significant and became stronger as social support increased (Fig. 4a).

The moderation analysis showed that social support also moderated the relationship between intra-SN connectivity and NA (T3) (interaction effect = −0.08, 95% CI = [−0.167, 0.002], $p = 0.05$). The results provided by the Johnson-Neyman analysis suggested that the relationship between intra-SN connectivity and NA (T3) was not significant for social support scores of 3.03 or below. Once social support scores passed this threshold, the relationship between intra-SN connectivity and NA (T3) was significant and became stronger as social support increased (Fig. 4b).

3.5. Exploratory analyses

Association between network connectivity and specific NA items at T2 and T3. Partial correlation analyses showed that most items were significantly associated with the current mean FNC (see Tables S3 and S4).

Sex differences in network connectivity associated with NA. Significant sex difference was not observed in the association between the NA scores and the FNCs, no matter what stage of the pandemic.

Association between whole brain network connectivity and NA. The analyses exploring the effects of whole-brain network connectivity patterns on NA are presented in Fig. S6. The results showed that the NA (T2) score was inversely associated with the intra-SN, intra-DMN, SN−FPN, SN−SMN, and DMN−DAN connectivity. Furthermore, the NA (T3) score was inversely associated with the intra-SN, SN−FPN, and FPN−SMN connectivity (FDR seed-level corrected $p < 0.05$, two-sided).

3.6. Sensitivity analyses

The analyses exploring the sensitivity and specificity of our original ROIs are presented in Fig. S4. The results showed that the NA (T2) score was inversely associated with the intra-SN, intra-DMN, intra-CEN, SN−DMN, SN−CEN, and DMN−CEN connectivity (FDR seed-level corrected $p < 0.05$, two-sided). Furthermore, the NA (T3) score was inversely associated with the intra-SN and SN−CEN connectivity (FDR seed-level corrected $p < 0.05$, two-sided).

4. Discussion

One of the novelties of the current study is the investigation of the protective factors of NA not only during the outbreak but also after the outbreak peak in China, which has significant implications for other countries that still have not reached theirs after peak. Our results are consistent with the prediction that the prevalence of negative emotion is higher during the pandemic than before the pandemic but does not decrease after the pandemic outbreak peak compared with during the pandemic, probably due to the far-reaching influences of COVID-19, such as economic uncertainty, fear of economic crisis and recession, and increased unemployment (Baker et al., 2020; Nicola et al., 2020). These aftereffects could all contribute to continuing NA after the actual pandemic peak (Y. Wang et al., 2020).

We also investigated the neurobiological relevance of NA under the COVID-19 outbreak, as well as the possible modulatory mechanisms of social support, in a large healthy sample. The results showed that inter-individual differences in NA related to COVID-19 were primarily predicted by rsFC within and between the SN (e.g., the amygdala, dACC, and SMG) and FPN (e.g., dlPFC), for which neural activity has been demonstrated to be associated with affective processing and executive function problems (J. Gong et al., 2018; Li et al., 2017; V. Menon, 2011; Palaniyappan and Liddle, 2013). The validity of the functional networks underlaying NA was tested using a machine-learning method. Notably, social support moderated the association between the network connectivity and NA, that is, individuals with a higher level of social support displayed the stronger correlations between intra-SN/SN−DMN connectivity and NA.

Our results showed that the greatest number of significantly correlated functional connections corresponded to the hubs of the SN. Consistently, studies have demonstrated that SN regional activity and connectivity between the SN and other brain regions are associated with anxiety (Roselinde H. Kaiser et al., 2015a,b), subjective emotional ratings (Seeley et al., 2007), and several affective disorders (Cullen et al., 2009; J. Gong et al., 2018; Horn et al., 2010; Sheline et al., 2010). Moreover, decreased connectivity between the SN and FPN is associated with increased repetitive negative emotion (Lydon-Staley et al., 2019) and greater impairment in emotion control (Andrei et al., 2013; Belleau et al., 2015; Ellard et al., 2018), suggesting that dysfunction of the SN and FPN is implicated in the circuitry responsible for behavior and emotion regulation (Q. Gong and He, 2015; Lui et al., 2011). Additionally, some regions in the SN and FPN, such as the amygdala (in the SN) and dlPFC (in the FPN), play a crucial role in predicting individual NA. The amygdala receives sensory information and processes social-emotional stimuli (Pang et al., 2016), while the dlPFC is believed to support top-down semantic assessment and alter the emotional responses of marginal areas using cognitive control (Drabant et al., 2009; Ochsner and Gross, 2005; Quirk and Beer, 2006). Specifically, coupling between the amygdala and dlPFC is considered the key to the theoretical models of emotion processing (John et al., 2013; Pang et al., 2016; Phelps, 2006). Notably, clinical studies have demonstrated that lower rsFC between the amygdala and prefrontal regions including the dlPFC

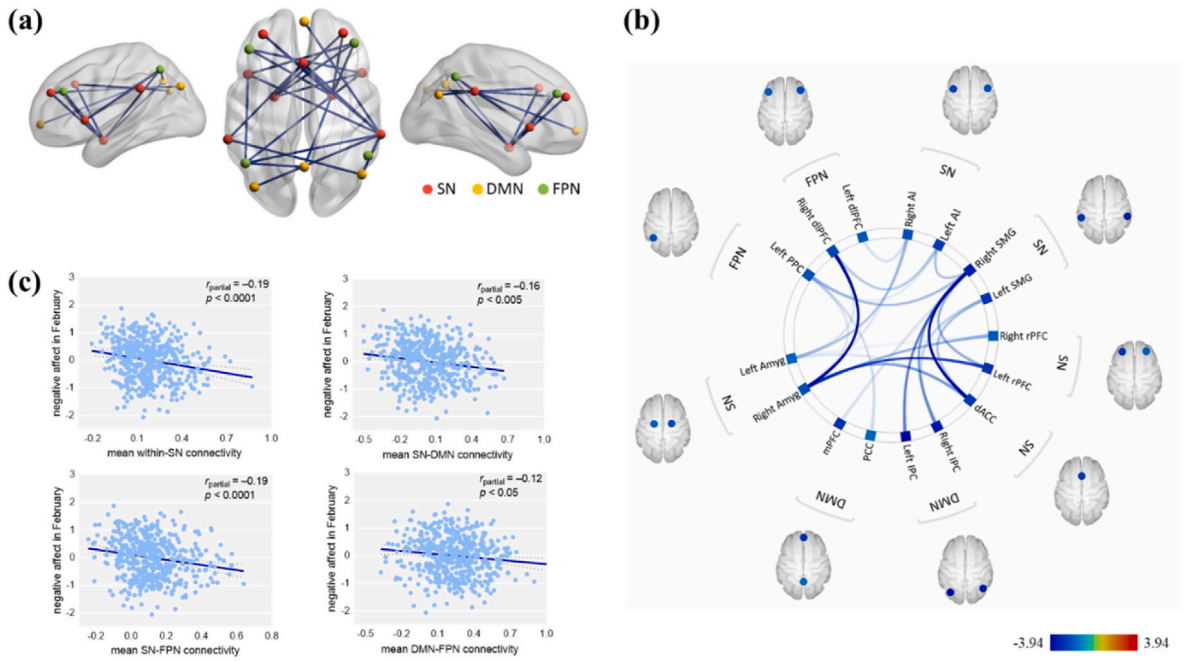

Fig. 1. Resting-state functional network connectivity of NA at T2. (a) Visual depiction of intra- and inter-network connectivity associated with the NA (T2) scores (FDR seed-level corrected $p < 0.05$, two-sided). (b) Connectivity patterns related to NA (T2) scores, as evidenced in this "connectome ring." (c) Scatter plots depicting the correlations between the NA (T2) scores and mean network connectivity strength after adjusting for age, sex, framewise displacement and NA level of scanning. Abbreviations: NA = negative affect; SN = salience network; DMN = default mode network; FPN = frontoparietal network; Amyg = amygdala; rPFC = rostral prefrontal cortex; dACC = dorsal anterior cingulate cortex; AI = anterior insula cortex; SMG = supramarginal gyrus; dlPFC = dorsolateral prefrontal cortex; PPC = posterior parietal cortex; mPFC = medial prefrontal cortex; PCC = posterior cingulate cortex; lPC = lateral parietal cortex.

Table 3
Functional connectivity within the SN and between SN and FPN: Negative correlations with NA (T3) scores[a].

Functional network connectivity	*t*-values	*p*-values[b]	Connectivity value (*Z*-scores)[c]
Within SN			
SN.Amyg (R)−SN.ACC	−2.96	0.0140	0.08 (±0.22)
SN.Amyg (R)−SN.rPFC (L)	−3.02	0.0140	−0.01 (±0.21)
SN.Amyg (R)−SN.rPFC (R)	−2.6	0.0245	−0.03 (±0.21)
Between SN and FPN			
SN.Amyg (R)−FPN.dlPFC (R)	−2.56	0.0245	0.03 (±0.20)
SN.Amyg (R)−FPN.PPC (L)	−3.01	0.0140	0.01 (±0.20)
SN.Amyg (R)−FPN.PPC (R)	−2.93	0.0140	−0.01 (±0.19)
SN.Amyg (R)−FPN.dlPFC (L)	−2.76	0.0192	0.05 (±0.21)

Abbreviations: NA = negative affect; SN = salience network; FPN = frontoparietal network; Amyg = amygdala; rPFC = rostral prefrontal cortex; dACC = dorsal anterior cingulate cortex; PPC = posterior parietal cortex; dlPFC = dorsolateral prefrontal cortex.

[a] Table 3 only shows the significant results (N = 496).

[b] False discovery rate (FDR) seed-level corrected $p < 0.05$, two-sided.

[c] Values are mean ± standard deviation (SD).

is associated with major depressive disorder and trait anxiety (Connolly et al., 2017; Pannekoek et al., 2014; Wheelock et al., 2014). Thus, given that the FCs within the SN and between the SN and FPN could negatively predict NA even after the outbreak peak, it appears plausible to suggest that increased involvement of SN-mediated emotion processing (e.g., emotion control, emotion regulation) manifesting as enhanced synchrony within the SN and between the SN and FPN may assuage negative emotions and help individuals to recover from the impact of the pandemic as soon as possible.

The current study also showed that SN–DMN connectivity could predict NA during the outbreak. Consistently, previous task-based studies also demonstrated the important role of SN–DMN connectivity on experimentally induced negative emotion responses (Habel et al., 2005; Harrison et al., 2008; Pelletier et al., 2003); individuals with greater connectivity between the amygdala and DMN during an unpleasant condition reported higher levels of trait reappraisal (Ferri et al., 2016), which is an important and efficient regulation strategy to reduce negative emotion rumination. Taken together, weak engagement of the DMN by SN might suggest the failure to adequately suppress DMN activity during emotional processing (L. Wang et al., 2017), and result in the altered self-referential mental activity (e.g., excessive rumination) (V. Menon, 2011), which might lead to the difficulties in adjusting perceptual and emotional responses to pandemic-related information and environmental changes in the early stages of the pandemic. We have also found the FC between PCC (in DMN) and PPC (in FPN) was negatively associated with NA (T2). Considering that this is the only significant result reported between DMN and FPN areas in the present sample, future researches are needed to explore this finding in an independent sample.

Further analysis results showed that social support moderated the relationship between SN connections and NA (T2 and T3). These results expanded the previous finding that social support could moderate the relationship between amygdala activation and anxiety (Hyde et al., 2011), suggesting that individuals with less social support might need greater activation in certain brain regions, such as the amygdala and prefrontal cortex, to regulate negative emotion (Schweizer et al., 2016). Additionally, accumulating studies have suggested that lower social support from family could persistently alter the neural circuitry of emotion regulation (McLaughlin et al., 2015; Moutsiana et al., 2014; Schweizer et al., 2016; Taylor et al., 2006). Thus, behavioral expressions of potential variability in brain function might be shaped by external factors, and the association between neural factors and behavior could be moderated by social context. Social support is also associated with the neural regions of threat processing and stress response, such as the amygdala, dACC, and AI (Eisenberger, 2013), as well as safety-related regions such as the ventromedial prefrontal cortex and PCC (Delgado et al., 2006; Schiller and Delgado, 2010), which might help people to face and process threat information during the pandemic. Moreover,

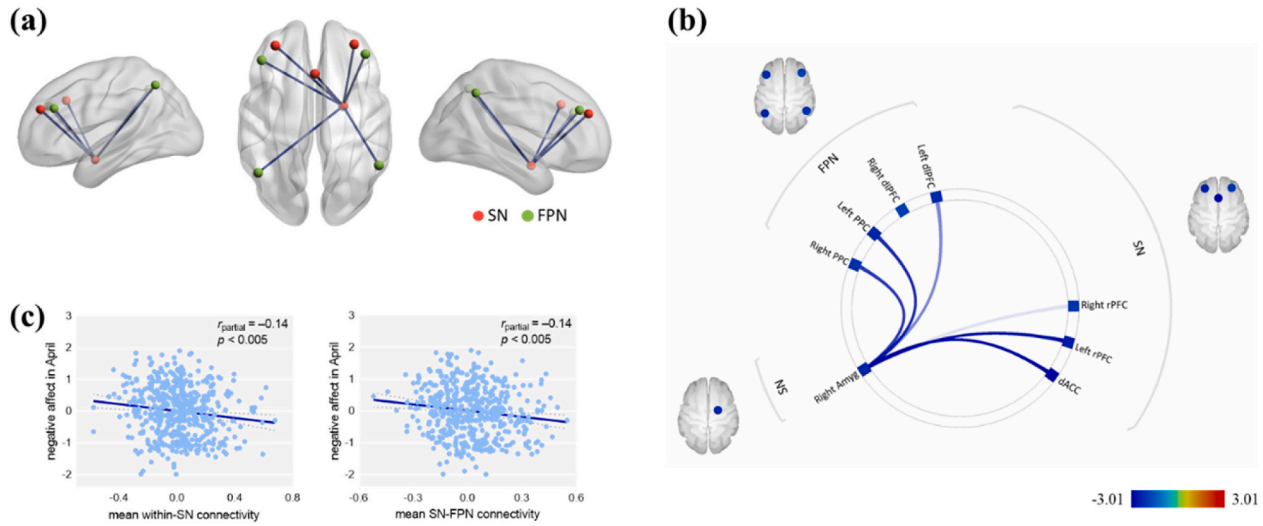

Fig. 2. Resting-state functional network connectivity of NA at T3. (a) Visual depiction of inter-network connectivity associated with the NA (T3) scores (FDR seed-level corrected $p < 0.05$, two-sided). (b) Connectivity patterns related to NA (T3) scores, as evidenced in this "connectome ring." (c) Scatter plots depicting the correlations between the NA (T3) scores and mean network connectivity strength after adjusting for age, sex, framewise displacement and NA level of scanning. Abbreviations: NA = negative affect; SN = salience network; FPN = frontoparietal network; Amyg = amygdala; rPFC = rostral prefrontal cortex; dACC = dorsal anterior cingulate cortex; PPC = posterior parietal cortex; dlPFC = dorsolateral prefrontal cortex.

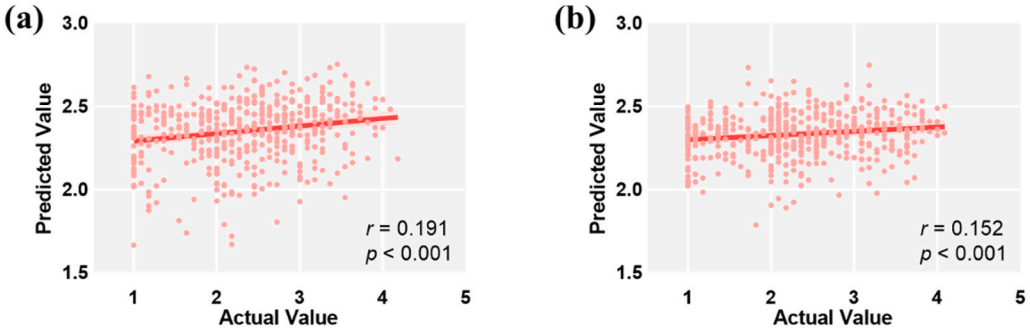

Fig. 3. The correlation between the actual value and predicted value of NA (T2) (a) and NA (T3) (b).

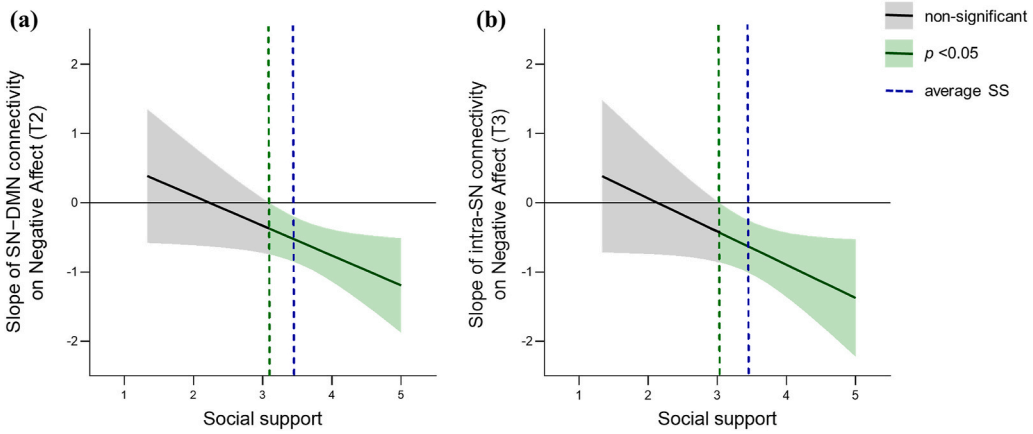

Fig. 4. Johnson-Neyman plots of social support where the slope between (a) SN−DMN connectivity and NA (T2) and (b) intra-SN connectivity and NA (T3) are significant. The green dashed line is the social support value at which the associations between network connectivity and NA were goes from nonsignificant (shaded gray area) to significant (shaded green area). The shaded area around the regression line is the 95% confidence interval. SS, social support. (For interpretation of the references to colour in this figure legend, the reader is referred to the Web version of this article.)

studies assessing perceptions of social support have found evidence for the "buffering" effect of social support (Cohen and Wills, 1985), suggesting that social support could predict more positive outcomes only during times of stress. Hence, the "buffering" effect might explain why the moderate effect of social support is significant but marginal on T3 ($p = 0.05$). The possible reason is that the peak of the COVID-19 epidemic in China has almost passed and the afraid emotion has abated, but the pressure still exists (see Table S1).

There are several limitations in our study that should be highlighted. First, because this study only included healthy participants, it remains unclear whether the results could be applied to clinical populations. Future studies with more diverse populations are necessary to confirm our present findings. Second, our fMRI data was collected before the outbreak. Further longitudinal MRI studies are needed to verify whether

there are any brain changes after the outbreak. Third, the study adopted self-reported NA scores. Other methods such as Ecological Momentary Assessment (Tennen et al., 2000) can be used to assess the NA level to minimize recall bias and maximize ecological validity.

5. Conclusions

In conclusion, the present results provided a crucial understanding of how neural network maps onto behavior under the environmental context, and they indicated that the SN and its interactions with the DMN and FPN plays the important role for people to adjust perceptual and emotional responses in the early stages of the pandemic, as well as to recover after the pandemic peak. Moreover, as a resource for coping with adversity, social support has promoted the expression and effect of the neural systems involved in salience and emotion processing, and buffered the negative emotional response under the uncertainty and stressful situation. Considering that the stress precipitated by the COVID-19 pandemic would be long-lasting, the powerful, inclusive, and enduring support from family and friends are crucial for individuals' better mental health.

CRediT authorship contribution statement

Mingyue Xiao: Conceptualization, Formal analysis, Supervision, Writing – original draft, Writing – review & editing. **Ximei Chen:** Conceptualization, Formal analysis, Supervision, Writing – review & editing. **Haijing Yi:** provided critical revisions, Writing – review & editing, Formal analysis. **Yijun Luo:** provided critical revisions, Writing – review & editing, Formal analysis. **Qiaoling Yan:** Writing – review & editing, Formal analysis. **Tingyong Feng:** approved the final version of the manuscript for submission. **Qinghua He:** approved the final version of the manuscript for submission. **Xu Lei:** provided the image data. **Jiang Qiu:** provided the image data. **Hong Chen:** Writing – original draft, provided critical revisions, provided the image data.

Declaration of competing interest

All authors reported no biomedical financial interests or potential conflicts of interest.

Acknowledgments

This study was funded by the National Natural Science Foundation of China (No. 31771237) and the Fundamental Research Funds for the Central Universities (No. SWU1709106). We would like to thank Editage (www.editage.cn) for English language editing.

Appendix A. Supplementary data

Supplementary data to this article can be found online at https://doi.org/10.1016/j.ynstr.2021.100418.

References

Andrei, M., Chun, M., Felix, B., Anselm, D., Masoud, T., Martin, S., Josef, B.U., 2013. Insular dysfunction within the salience network is associated with severity of symptoms and aberrant inter-network connectivity in major depressive disorder. Front. Human Neuroence 7, 930.

Andrews-Hanna, J.R., 2012. The brain's default network and its adaptive role in internal mentation. Neuroscientist 18 (3), 251–270.

Ashburner, J., 2007. A fast diffeomorphic image registration algorithm. Neuroimage 38 (1), 95–113. https://doi.org/10.1016/j.neuroimage.2007.07.007. Retrieved from. http://www.sciencedirect.com/science/article/pii/S1053811907005848.

Baker, S.R., Bloom, N., Davis, S.J., Terry, S.J., 2020. Covid-induced Economic Uncertainty (Retrieved from).

Beaty, R.E., Kenett, Y.N., Christensen, A.P., Rosenberg, M.D., Benedek, M., Chen, Q., Kane, M.J., 2018. Robust prediction of individual creative ability from brain functional connectivity. Proc. Natl. Acad. Sci. Unit. States Am. 115 (5), 1087–1092.

Belleau, E.L., Taubitz, L.E., Larson, C.L., 2015. Imbalance of default mode and regulatory networks during externally focused processing in depression. Soc. Cognit. Affect Neurosci. 10 (5), 744–751. https://doi.org/10.1093/scan/nsu117. Retrieved from, doi:10.1093/scan/nsu117.

Biswal, B.B., 2012. Resting state fMRI: a personal history. Neuroimage 62 (2), 938–944. https://doi.org/10.1016/j.neuroimage.2012.01.090. Retrieved from. http://www.sciencedirect.com/science/article/pii/S1053811912001073.

Chahal, R., Kirshenbaum, J.S., Miller, J.G., Ho, T.C., Gotlib, I.H., 2021. Higher executive control network coherence buffers against puberty-related increases in internalizing symptoms during the COVID-19 pandemic. Biol. Psychiatr.: Cogn. Neurosci. Neuroimag. 6 (1), 79–88.

Chen, X., Gao, X., Qin, J., Wang, C., Xiao, M., Tian, Y., He, Q., 2021. Resting-state functional network connectivity underlying eating disorder symptoms in healthy young adults. Neuroimage: Clin. 30, 102671.

Cohen, S., McKay, G., 2020. Social support, stress and the buffering hypothesis: a theoretical analysis. In: Handbook of Psychology and Health, ume IV. Routledge, pp. 253–267.

Cohen, S., Wills, T.A., 1985. Stress, social support, and the buffering hypothesis. Psychol. Bull. 98 (2), 310.

Connolly, C.G., Ho, T.C., Blom, E.H., LeWinn, K.Z., Sacchet, M.D., Tymofiyeva, O., Yang, T.T., 2017. Resting-state functional connectivity of the amygdala and longitudinal changes in depression severity in adolescent depression. J. Affect. Disord. 207, 86–94. Retrieved from. http://www.sciencedirect.com/science/article/pii/S0165032716310540. https://doi.org/10.1016/j.jad.2016.09.026.

Craig, A.D., 2009. Emotional moments across time: a possible neural basis for time perception in the anterior insula. Phil. Trans. Biol. Sci. 364 (1525), 1933–1942. https://doi.org/10.1098/rstb.2009.0008. Retrieved from, 10.1098/rstb.2009.0008.

Cui, Z., Su, M., Li, L., Shu, H., Gong, G., 2018. Individualized prediction of reading comprehension ability using gray matter volume. Cerebr. Cortex 28 (5), 1656–1672.

Cullen, K.R., Gee, D.G., Klimes-Dougan, B., Gabbay, V., Hulvershorn, L., Mueller, B.A., Milham, M.P., 2009. A preliminary study of functional connectivity in comorbid adolescent depression. Neurosci. Lett. 460 (3), 227–231. Retrieved from. http://www.sciencedirect.com/science/article/pii/S0304394009006478, 10.1016/j.neulet.2009.05.022.

d'Arbeloff, T.C., Freedy, K.R., Knodt, A.R., Radtke, S.R., Brigidi, B.D., Hariri, A.R., 2018. Emotion regulation and the experience of future negative mood: the importance of assessing social support. Front. Psychol. 9, 2287.

Delgado, M.R., Olsson, A., Phelps, E.A., 2006. Extending animal models of fear conditioning to humans. Biol. Psychol. 73 (1), 39–48.

Desikan, R.S., Ségonne, F., Fischl, B., Quinn, B.T., Dickerson, B.C., Blacker, D., Hyman, B. T., 2006. An automated labeling system for subdividing the human cerebral cortex on MRI scans into gyral based regions of interest. Neuroimage 31 (3), 968–980.

Dijk, K.R.A.V., Hedden, T., Venkataraman, A., Evans, K.C., Lazar, S.W., Buckner, R.L., 2010. Intrinsic functional connectivity as a tool for human connectomics: theory, properties, and optimization. J. Neurophysiol. 103 (1), 297–321. Retrieved from. https://journals.physiology.org/doi/abs/10.1152/jn.00783, 2009, 10.1152/jn.00783.2009.

Domakonda, M.J., He, X., Lee, S., Cyr, M., Marsh, R., 2019. Increased functional connectivity between ventral attention and default mode networks in adolescents with bulimia nervosa. J. Am. Acad. Child Adolesc. Psychiatr. 58 (2), 232–241.

Drabant, E.M., McRae, K., Manuck, S.B., Hariri, A.R., Gross, J.J., 2009. Individual differences in typical reappraisal use predict amygdala and prefrontal responses. Biol. Psychiatr. 65 (5), 367–373. Retrieved from. http://www.sciencedirect.com/science/article/pii/S0006322308010986. https://doi.org/10.1016/j.biopsych.2008.09.007.

Eisenberger, N.I., 2013. An empirical review of the neural underpinnings of receiving and giving social support: implications for health. Psychosom. Med. 75 (6), 545.

Ellard, K.K., Zimmerman, J.P., Kaur, N., Van Dijk, K.R.A., Roffman, J.L., Nierenberg, A. A., Camprodon, J.A., 2018. Functional connectivity between anterior insula and key nodes of frontoparietal executive control and salience networks distinguish bipolar depression from unipolar depression and healthy control subjects. Biol. Psychiatr.: Cogn. Neurosci. Neuroimag. 3 (5), 473–484. Retrieved from. http://www.sciencedirect.com/science/article/pii/S2451902218300272. https://doi.org/10.1016/j.bpsc.2018.01.013.

Elmira, I., Jessica, D.S., Jean-Philippe, G., Pomares, F.B., Frank, V., Tremblay, R.E., Linda, B., 2018. Associations between daily mood states and brain gray matter volume, resting-state functional connectivity and task-based activity in healthy adults. Front. Human Neuroence 12, 168.

Ferri, J., Schmidt, J., Hajcak, G., Canli, T., 2016. Emotion regulation and amygdala-precuneus connectivity: focusing on attentional deployment. Cognit. Affect Behav. Neurosci. 16 (6), 991–1002. https://doi.org/10.3758/s13415-016-0447-y. Retrieved from, doi:10.3758/s13415-016-0447-y.

Friston, K.J., Williams, S., Howard, R., Frackowiak, R.S.J., Turner, R., 1996. Movement-Related effects in fMRI time-series. Magn. Reson. Med. 35 (3), 346–355. https://doi.org/10.1002/mrm.1910350312.

Galea, S., Merchant, R.M., Lurie, N., 2020. The mental health consequences of COVID-19 and physical distancing: the need for prevention and early intervention. JAMA Intern. Med. 180 (6), 817–818.

Giesbrecht, G.F., Poole, J.C., Letourneau, N., Campbell, T., Kaplan, B.J., Team, A.S., 2013. The buffering effect of social support on hypothalamic-pituitary-adrenal axis function during pregnancy. Psychosom. Med. 75 (9), 856–862.

Gong, J., Chen, G., Jia, Y., Zhong, S., Zhao, L., Luo, X., Huang, L., 2018. Disrupted functional connectivity within the default mode network and salience network in unmedicated bipolar II disorder. Prog. Neuro Psychopharmacol. Biol. Psychiatr. 88, 11–18.

Gong, Q., He, Y., 2015. Depression, neuroimaging and connectomics: a selective overview. Biol. Psychiatr. 77 (3), 223–235. Retrieved from. http://www.sciencedirect.com/science/article/pii/S000632231400609X. https://doi.org/10.1016/j.biopsych.2014.08.009.

Greicius, M.D., Krasnow, B., Reiss, A.L., Menon, V., 2003. Functional connectivity in the resting brain: a network analysis of the default mode hypothesis. Proc. Natl. Acad. Sci. Unit. States Am. 100 (1), 253–258.

Gunnell, D., Appleby, L., Arensman, E., Hawton, K., John, A., Kapur, N., Caine, E.D., 2020. Suicide risk and prevention during the COVID-19 pandemic. Lancet Psychiatr. 7 (6), 468–471.

Habel, U., Klein, M., Kellermann, T., Shah, N.J., Schneider, F., 2005. Same or different? Neural correlates of happy and sad mood in healthy males. Neuroimage 26 (1), 206–214. Retrieved from. http://www.sciencedirect.com/science/article/pii/S1053811905000406. https://doi.org/10.1016/j.neuroimage.2005.01.014.

Hallquist, M.N., Hwang, K., Luna, B., 2013. The nuisance of nuisance regression: spectral misspecification in a common approach to resting-state fMRI preprocessing reintroduces noise and obscures functional connectivity. Neuroimage 82, 208–225. Retrieved from. http://www.sciencedirect.com/science/article/pii/S1053811913006265. https://doi.org/10.1016/j.neuroimage.2013.05.116.

Hampson, M., Driesen, N., Roth, J.K., Gore, J.C., Constable, R.T., 2010. Functional connectivity between task-positive and task-negative brain areas and its relation to working memory performance. Magn. Reson. Imag. 28 (8), 1051–1057.

Harrison, B.J., Pujol, J., Ortiz, H., Fornito, A., Pantelis, C., Yücel, M., 2008. Modulation of brain resting-state networks by sad mood induction. PLoS One 3 (3), e1794. https://doi.org/10.1371/journal.pone.0001794. Retrieved from, 10.1371/journal.pone.0001794.

Hayes, A.F., 2013. Introduction to Mediation, Moderation, and Conditional Process Analysis: A Regression-Based Approach.

Hayes, A.F., Matthes, J., 2009. Computational procedures for probing interactions in OLS and logistic regression: SPSS and SAS implementations. Behav. Res. Methods 41 (3), 924–936.

He, L., Wei, D., Yang, F., Zhang, J., Cheng, W., Feng, J., Ren, Z., 2021. Functional connectome prediction of anxiety related to the COVID-19 pandemic. Am. J. Psychiatr. appi. ajp. 2020.20070979.

He, Z., Lu, F., Sheng, W., Han, S., Long, Z., Chen, Y., Chen, H., 2019. Functional dysconnectivity within the emotion-regulating system is associated with affective symptoms in major depressive disorder: a resting-state fMRI study. Aust. N. Z. J. Psychiatr. 53 (6), 528–539. Retrieved from. https://journals.sagepub.com/doi/abs/10.1177/0004867419832106, 10.1177/0004867419832106.

Holmes, E.A., O'Connor, R.C., Perry, V.H., Tracey, I., Wessely, S., Arseneault, L., Everall, I., 2020. Multidisciplinary research priorities for the COVID-19 pandemic: a call for action for mental health science. Lancet Psychiatr. 7 (6), 547–560.

Horn, D.I., Yu, C., Steiner, J., Buchmann, J., Walter, M., 2010. Glutamatergic and resting-state functional connectivity correlates of severity in major depression – the role of pregenual anterior cingulate cortex and anterior insula. Front. Syst. Neuroen. 4.

Hyde, L.W., Gorka, A., Manuck, S.B., Hariri, A.R., 2011. Perceived social support moderates the link between threat-related amygdala reactivity and trait anxiety. Neuropsychologia 49 (4), 651–656.

Jackson, T., Chen, H., 2015. Features of objectified body consciousness and sociocultural perspectives as risk factors for disordered eating among late-adolescent women and men. J. Counsel. Psychol. 62 (4), 741–752. https://doi.org/10.1037/cou0000096.

John, Y.J., Daniel, B., Basilis, Z., Helen, B., 2013. Anatomy and computational modeling of networks underlying cognitive-emotional interaction. Front. Human Neuroence 7 (101), 101.

Johnstone, T., van Reekum, C.M., Urry, H.L., Kalin, N.H., Davidson, R.J., 2007. Failure to regulate: counterproductive recruitment of top-down prefrontal-subcortical circuitry in major depression. J. Neurosci. 27 (33), 8877. Retrieved from. http://www.jneurosci.org/content/27/33/8877.abstract, 10.1523/JNEUROSCI.2063-07.2007.

Kaiser, R.H., Andrews-Hanna, J.R., Spielberg, J.M., Warren, S.L., Sutton, B.P., Miller, G.A., Banich, M.T., 2015a. Distracted and down: neural mechanisms of affective interference in subclinical depression. Soc. Cognit. Affect Neurosci. 10 (5), 654–663.

Kaiser, R.H., Andrews-Hanna, J.R., Wager, T.D., Pizzagalli, D.A., 2015b. Large-scale network dysfunction in major depressive disorder: a meta-analysis of resting-state functional connectivity. JAMA Psychiatry 72 (6), 603–611. https://doi.org/10.1001/jamapsychiatry.2015.0071. Retrieved from, 10.1001/jamapsychiatry.2015.0071.

Kerns, J.G., Cohen, J.D., MacDonald, A.W., Johnson, M.K., Stenger, V.A., Aizenstein, H., Carter, C.S., 2005. Decreased conflict- and error-related activity in the anterior cingulate cortex in subjects with schizophrenia. Am. J. Psychiatr. 162 (10), 1833–1839. https://doi.org/10.1176/appi.ajp.162.10.1833. Retrieved from, 10.1176/appi.ajp.162.10.1833.

Kunisato, Y., Okamoto, Y., Okada, G., Aoyama, S., Nishiyama, Y., Onoda, K., Yamawaki, S., 2011. Personality traits and the amplitude of spontaneous low-frequency oscillations during resting state. Neurosci. Lett. 492 (2), 109–113. Retrieved from. http://www.sciencedirect.com/science/article/pii/S0304394011001133. https://doi.org/10.1016/j.neulet.2011.01.067.

Lei, X., Yang, T., Wu, T., 2015. Functional neuroimaging of extraversion-introversion. Neurosci. Bull. 31 (6), 663–675.

Li, M., Das, T., Deng, W., Wang, Q., Li, Y., Zhao, L., Li, T., 2017. Clinical utility of a short resting-state MRI scan in differentiating bipolar from unipolar depression. Acta Psychiatr. Scand. 136 (3), 288–299. Retrieved from. https://onlinelibrary.wiley.com/doi/abs/10.1111/acps.12752. https://doi.org/10.1111/acps.12752.

Liu, P., Yang, W., Zhuang, K., Wei, D., Yu, R., Huang, X., Qiu, J., 2021. The functional connectome predicts feeling of stress on regular days and during the COVID-19 pandemic. Neurobiol. Stress 14, 100285.

Lui, S., Wu, Q., Qiu, L., Yang, X., Kuang, W., Chan, R.C.K., Gong, Q., 2011. Resting-state functional connectivity in treatment-resistant depression. Am. J. Psychiatr. 168 (6), 642–648. https://doi.org/10.1176/appi.ajp.2010.10101419. Retrieved from, 10.1176/appi.ajp.2010.10101419.

Lydon-Staley, D.M., Kuehner, C., Zamoscik, V., Huffziger, S., Kirsch, P., Bassett, D.S., 2019. Repetitive negative thinking in daily life and functional connectivity among default mode, fronto-parietal, and salience networks. Transl. Psychiatry 9 (1), 234. https://doi.org/10.1038/s41398-019-0560-0. Retrieved from, 10.1038/s41398-019-0560-0.

Mahadevan, A.S., Tooley, U.A., Bertolero, M.A., Mackey, A.P., Bassett, D.S., 2021. Evaluating the sensitivity of functional connectivity measures to motion artifact in resting-state fMRI data. Neuroimage 241, 118408.

McLaughlin, K.A., Peverill, M., Gold, A.L., Alves, S., Sheridan, M.A., 2015. Child maltreatment and neural systems underlying emotion regulation. J. Am. Acad. Child Adolesc. Psychiatr. 54 (9), 753–762.

Menon, B., 2019. Towards a new model of understanding–The triple network, psychopathology and the structure of the mind. Med. Hypotheses 133, 109385.

Menon, V., 2011. Large-scale brain networks and psychopathology: a unifying triple network model. Trends Cogn. Sci. 15 (10), 483–506.

Michalak, E.E., Wilkinson, C., Hood, K., Dowrick, C., Wilkinson, G., 2003. Seasonality, negative life events and social support in a community sample. Br. J. Psychiatry 182 (5), 434–438. Retrieved from. https://www.cambridge.org/core/article/seasonality-negative-life-events-and-social-support-in-a-community-sample/3978C938D38BE6B611E4FE15273F81B0, 10.1192/bjp.182.5.434.

Miller, E.K., Cohen, J.D., 2001. An integrative theory of prefrontal cortex function. Annu. Rev. Neurosci. 24 (1), 167–202.

Moutsiana, C., Fearon, P., Murray, L., Cooper, P., Goodyer, I., Johnstone, T., Halligan, S., 2014. Making an effort to feel positive: insecure attachment in infancy predicts the neural underpinnings of emotion regulation in adulthood. JCPP (J. Child Psychol. Psychiatry) 55 (9), 999–1008.

Nicola, M., Alsafi, Z., Sohrabi, C., Kerwan, A., Al-Jabir, A., Iosifidis, C., Agha, R., 2020. The socio-economic implications of the coronavirus pandemic (COVID-19): a review. Int. J. Surg. 78, 185–193.

Ochsner, K.N., Gross, J.J., 2005. The cognitive control of emotion. Trends Cognit. Sci. 9 (5), 242–249. Retrieved from. http://www.sciencedirect.com/science/article/pii/S1364661305000902. https://doi.org/10.1016/j.tics.2005.03.010.

Ozbay, F., Johnson, D.C., Dimoulas, E., Morgan III, C., Charney, D., Southwick, S., 2007. Social support and resilience to stress: from neurobiology to clinical practice. Psychiatry (Edgmont) 4 (5), 35.

Palaniyappan, L., Liddle, P.F., 2013. Diagnostic discontinuity in psychosis: a combined study of cortical gyrification and functional connectivity. Schizophr. Bull. 40 (3), 675–684. https://doi.org/10.1093/schbul/sbt050. Retrieved from, doi:10.1093/schbul/sbt050.

Palinkas, L.A., Johnson, J.C., Boster, J.S., 2004. Social support and depressed mood in isolated and confined environments. Acta Astronaut. 54 (9), 639–647.

Pang, Y., Cui, Q., Wang, Y., Chen, Y., Wang, X., Han, S., Chen, H., 2016. Extraversion and neuroticism related to the resting-state effective connectivity of amygdala. Sci. Rep. 6 (1), 35484. https://doi.org/10.1038/srep35484. Retrieved from, 10.1038/srep.35484.

Pannekoek, J.N., van der Werff, S.J.A., Meens, P.H.F., van den Bulk, B.G., Jolles, D.D., Veer, I.M., Vermeiren, R.R.J.M., 2014. Aberrant resting-state functional connectivity in limbic and salience networks in treatment-naïve clinically depressed adolescents. JCPP (J. Child Psychol. Psychiatry) 55 (12), 1317–1327. Retrieved from. https://acamh.onlinelibrary.wiley.com/doi/abs/10.1111/jcpp.12266. https://doi.org/10.1111/jcpp.12266.

Pelletier, M., Bouthillier, A., Lévesque, J., Carrier, S., Breault, C., Paquette, V., Beauregard, M., 2003. Separate neural circuits for primary emotions? Brain activity during self-induced sadness and happiness in professional actors. Neuroreport 14 (8), 1111–1116. Retrieved from. https://journals.lww.com/neuroreport/Fulltext/2003/06110/Separate_neural_circuits_for_primary_emotions_.3.aspx.

Phelps, E.A., 2006. Emotion and cognition: insights from studies of the human amygdala. Annu. Rev. Psychol. 57 (1), 27–53. Retrieved from. https://www.annualreviews.org/doi/abs/10.1146/annurev.psych.56.091103.070234, 10.1146/annurev.psych.56.091103.070234.

Puterman, E., Epel, E.S., O'Donovan, A., Prather, A.A., Aschbacher, K., Dhabhar, F.S., 2014. Anger is associated with increased IL-6 stress reactivity in women, but only among those low in social support. Int. J. Behav. Med. 21 (6), 936–945.

Qian, M., Wu, Q., Wu, P., Hou, Z., Liang, Y., Cowling, B.J., Yu, H., 2020. Psychological Responses, Behavioral Changes and Public Perceptions during the Early Phase of the COVID-19 Outbreak in China: a Population Based Cross-Sectional Survey. medRxiv.

Quirk, G.J., Beer, J.S., 2006. Prefrontal involvement in the regulation of emotion: convergence of rat and human studies. Curr. Opin. Neurobiol. 16 (6), 723–727. Retrieved from. http://www.sciencedirect.com/science/article/pii/S0959438806001383. https://doi.org/10.1016/j.conb.2006.07.004.

Raichle, M.E., MacLeod, A.M., Snyder, A.Z., Powers, W.J., Gusnard, D.A., Shulman, G.L., 2001. A default mode of brain function. Proc. Natl. Acad. Sci. Unit. States Am. 98 (2), 676–682.

Ren, Y., Qian, W., Li, Z., Liu, Z., Zhou, Y., Wang, R., Zhang, X., 2020. Public mental health under the long-term influence of COVID-19 in China: geographical and temporal distribution. J. Affect. Disord. 277, 893–900. Retrieved from. http://www.sciencedirect.com/science/article/pii/S0165032720326513. https://doi.org/10.1016/j.jad.2020.08.045.

Resick, P.A., 2001. Stress and Trauma. Psychology Press.

Schiller, D., Delgado, M.R., 2010. Overlapping neural systems mediating extinction, reversal and regulation of fear. Trends Cognit. Sci. 14 (6), 268–276.

Schmidt, A.T., Hanten, G.R., Li, X., Orsten, K.D., Levin, H.S., 2010a. Emotion recognition following pediatric traumatic brain injury: longitudinal analysis of emotional prosody and facial emotion recognition. Neuropsychologia 48 (10), 2869–2877.
Schmidt, A.T., Orsten, K.D., Hanten, G.R., Li, X., Levin, H.S., 2010b. Family environment influences emotion recognition following paediatric traumatic brain injury. Brain Inj. 24 (13–14), 1550–1560.
Schouten, T.M., Koini, M., De Vos, F., Seiler, S., Van Der Grond, J., Lechner, A., De Rooij, M., 2016. Combining anatomical, diffusion, and resting state functional magnetic resonance imaging for individual classification of mild and moderate Alzheimer's disease. Neuroimage: Clin. 11, 46–51.
Schweizer, S., Walsh, N.D., Stretton, J., Dunn, V.J., Goodyer, I.M., Dalgleish, T., 2016. Enhanced emotion regulation capacity and its neural substrates in those exposed to moderate childhood adversity. Soc. Cognit. Affect Neurosci. 11 (2), 272–281.
Seeley, W.W., Menon, V., Schatzberg, A.F., Keller, J., Glover, G.H., Kenna, H., et al., 2007. Dissociable intrinsic connectivity networks for salience processing and executive control. J. Neurosci. 27 (9), 2349–2356.
Seth, A.K., 2005. Causal connectivity of evolved neural networks during behavior. Netw. Comput. Neural Syst. 16 (1), 35–54.
Sheline, Y.I., Price, J.L., Yan, Z., Mintun, M.A., 2010. Resting-state functional MRI in depression unmasks increased connectivity between networks via the dorsal nexus. Proc. Natl. Acad. Sci. Unit. States Am. 107 (24), 11020. Retrieved from. http://www.pnas.org/content/107/24/11020.abstract, 10.1073/pnas.1000446107.
Shen, W., Tu, Y., Gollub, R.L., Ortiz, A., Napadow, V., Yu, S., Jung, M., 2019. Visual network alterations in brain functional connectivity in chronic low back pain: a resting state functional connectivity and machine learning study. Neuroimage: Clin. 22, 101775.
Shen, X., Finn, E.S., Scheinost, D., Rosenberg, M.D., Chun, M.M., Papademetris, X., Constable, R.T., 2017. Using connectome-based predictive modeling to predict individual behavior from brain connectivity. Nat. Protoc. 12 (3), 506–518.
Shirer, W.R., Ryali, S., Rykhlevskaia, E., Menon, V., Greicius, M.D., 2012. Decoding subject-driven cognitive states with whole-brain connectivity patterns. Cerebr. Cortex 22 (1), 158–165.
Spiller, S.A., Fitzsimons, G.J., Lynch Jr., J.G., McClelland, G.H., 2013. Spotlights, floodlights, and the magic number zero: simple effects tests in moderated regression. J. Market. Res. 50 (2), 277–288.
Supekar, K., Swigart, A.G., Tenison, C., Jolles, D.D., Rosenberg-Lee, M., Fuchs, L., Menon, V., 2013. Neural predictors of individual differences in response to math tutoring in primary-grade school children. Proc. Natl. Acad. Sci. Unit. States Am. 110 (20), 8230. Retrieved from. http://www.pnas.org/content/110/20/8230.abstract, 10.1073/pnas.1222154110.
Taylor, S.E., Eisenberger, N.I., Saxbe, D., Lehman, B.J., Lieberman, M.D., 2006. Neural responses to emotional stimuli are associated with childhood family stress. Biol. Psychiatr. 60 (3), 296–301.
Tennen, H., Affleck, G., Armeli, S., Carney, M.A., 2000. A daily process approach to coping: linking theory, research, and practice. Am. Psychol. 55 (6), 626.
Tie, Y., Rigolo, L., Ozdemir Ovalioglu, A., Olubiyi, O., Doolin, K.L., Mukundan Jr., S., Golby, A.J., 2015. A new paradigm for individual subject language mapping: movie-watching fMRI. J. Neuroimaging 25 (5), 710–720.
Van Duijvenvoorde, A.C., Westhoff, B., de Vos, F., Wierenga, L.M., Crone, E.A., 2019. A three-wave longitudinal study of subcortical–cortical resting-state connectivity in adolescence: testing age-and puberty-related changes. Hum. Brain Mapp. 40 (13), 3769–3783.
Varoquaux, G., Raamana, P.R., Engemann, D.A., Hoyos-Idrobo, A., Schwartz, Y., Thirion, B., 2017. Assessing and tuning brain decoders: cross-validation, caveats, and guidelines. Neuroimage 145, 166–179.
Veer, I.M., Oei, N.Y., Spinhoven, P., van Buchem, M.A., Elzinga, B.M., Rombouts, S.A., 2011. Beyond acute social stress: increased functional connectivity between amygdala and cortical midline structures. Neuroimage 57 (4), 1534–1541.
Wang, C., Pan, R., Wan, X., Tan, Y., Xu, L., McIntyre, R.S., Sharma, V.K., 2020. A longitudinal study on the mental health of general population during the COVID-19 epidemic in China. Brain Behav. Immun. 87, 40–48.
Wang, L., Shen, H., Lei, Y., Zeng, L.-L., Cao, F., Su, L., Hu, D., 2017. Altered default mode, fronto-parietal and salience networks in adolescents with Internet addiction. Addict. Behav. 70, 1–6. Retrieved from. http://www.sciencedirect.com/science/article/pii/S0306460317300308. https://doi.org/10.1016/j.addbeh.2017.01.021.
Wang, X., Wang, X., Ma, H., 1999. Handbook of Mental Health Assessment Scale; Chin. Ment. Health Press, Beijing, China, pp. 131–133.
Wang, Y., Hu, Z., Feng, Y., Wilson, A., Chen, R., 2020. Changes in network centrality of psychopathology symptoms between the COVID-19 outbreak and after peak. Mol. Psychiatr. 25 (12), 3140–3149.
Watson, D., Clark, L.A., Tellegen, A., 1988. Development and validation of brief measures of positive and negative affect: the PANAS scales. J. Pers. Soc. Psychol. 54 (6), 1063–1070.
Wehrle, F.M., Michels, L., Guggenberger, R., Huber, R., Latal, B., O'Gorman, R.L., Hagmann, C.F., 2018. Altered resting-state functional connectivity in children and adolescents born very preterm short title. Neuroimage: Clin. 20, 1148–1156.
Wheelock, M.D., Sreenivasan, K.R., Wood, K.H., Ver Hoef, L.W., Deshpande, G., Knight, D.C., 2014. Threat-related learning relies on distinct dorsal prefrontal cortex network connectivity. Neuroimage 102, 904–912. Retrieved from. http://www.sciencedirect.com/science/article/pii/S1053811914006557. https://doi.org/10.1016/j.neuroimage.2014.08.005.
Whitfield-Gabrieli, S., Nieto-Castanon, A., 2012. Conn: a functional connectivity toolbox for correlated and anticorrelated brain networks. Brain Connect. 2 (3), 125–141.
Xu, J., Van Dam, N.T., Feng, C., Luo, Y., Ai, H., Gu, R., Xu, P., 2019. Anxious brain networks: a coordinate-based activation likelihood estimation meta-analysis of resting-state functional connectivity studies in anxiety. Neurosci. Biobehav. Rev. 96, 21–30. Retrieved from. http://www.sciencedirect.com/science/article/pii/S0149763418304123. https://doi.org/10.1016/j.neubiorev.2018.11.005.
Yan, C.-G., Wang, X.-D., Zuo, X.-N., Zang, Y.-F., 2016. DPABI: data processing & analysis for (Resting-State) brain imaging. Neuroinformatics 14 (3), 339–351. https://doi.org/10.1007/s12021-016-9299-4. Retrieved from, 10.1007/s12021-016-9299-4.
Yarkoni, T., Westfall, J., 2017. Choosing prediction over explanation in psychology: lessons from machine learning. Perspect. Psychol. Sci. 12 (6), 1100–1122.